Sand Provenance from Major and Trace Element Analyses
of Bulk Rock and Sand Grains

P. Armienti[1], B. Messiga[2] & R. Vannucci[2]

[1]Dipartimento di Scienze della Terra, Università di Pisa, Via S. Maria 53, I-56126 Pisa - Italy
[2]Dipartimento di Scienze della Terra, Università di Pavia, Via Ferrata 1, I-27100 Pavia - Italy

Abstract - Thirty-nine medium and fine grained sandstones from between 19.26 and 147.23 mbsf in the Cape Roberts-1 core (CRP-1) were analysed for 10 major and 16 trace elements. Using whole-rock compositions, 9 samples were selected for analyses of mineral and glass grains by energy dispersive electron microscope. Laser-Ablation Mass-Spectrometry was used to determine rare earth elements and 14 additional trace elements in glass shards, pyroxenes and feldspars in order to examine their contribution to the bulk rock chemistry. Geochemical data reveal the major contribution played by the Granite Harbour Intrusives to the whole rock composition, even if a significant input is supplied by McMurdo volcanics and Ferrar dolerite pyroxenes. McMurdo volcanics were studied in detail; they appear to derive from a variety of litologies, and a dominant role of wind transportation from exposures of volcanic rocks may be inferred from the contemporary occurrence of different compositions at all depths. Only at 116.55 mbsf was a thin layer of tephra found, linked to an explosive eruption. McMurdo volcanic rocks exhibit larger abundances at depths above 62 mbsf, in correspondence with the onset of volcanic activity in the McMurdo Sound area. From 62 mbsf to the bottom of the core, McMurdo volcanics are less abundant and probably issued from some centres in the McMurdo Sound region. However, available data do not allow the exclusion of wind transport from some eruptive centres active in north Victoria Land at the beginning of the Miocene Epoch.
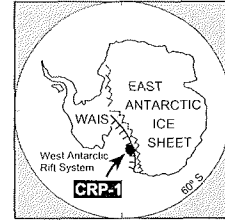
INTRODUCTION

The sandstone samples examined in this study all belong to Quaternary and Miocene sediments. In this time-span the area of Victoria Land immediately adjacent to the Cape Roberts area has remained practically in its present state (Hall et al., 1997). Thus the immediate hinterland of the drill-site may have provided only minor amounts of debris to the CRP-1 site, due to the lack of glaciers draining the Dry Valleys region. MacKay Glacier, Ferrar Glacier and other Polar Plateau outlet glaciers, as a result of longshore drift and additional ice-borne and air-borne debris, thus represent the main sources of sediments at the drillsite. All possible conclusions derived form the following mineralogical and geochemical data need to be considered in the context of this palaeodrainage pattern and will mainly provide information about the catchments of those glaciers.

PETROGRAPHIC DATA

Textural and modal data on the same set of samples examined in this work are described by Smellie (this volume). All the samples (Tab. 1) are sandstones even when collected from units of variable grain size. The uniform grain size minimises the influence of mean grain size on the bulk chemistry (Roser & Pyne, 1989). Detrital grains represent variable amounts in the different samples, reaching values of up 90%. Matrix usually becomes more abundant in the finer grained varieties (Smellie, this volume; De Santis & Barrett, this volume). Quartz and feldspars may form up to 60-80% of detrital grains. Quartz is the dominant mineral in the sand mode, and is mainly represented by angular and subangular fragments. Abraded, rounded grains are also abundant, together with polycrystalline grains in which quartz is often associated with alkali feldspars (Smellie, this volume). Alkali feldspar (orthoclase, less abundant microcline and minor sanidine and/or anorthoclase) is the second dominant phase. Pale green pyroxene is the most common ferromagnesian mineral; it occurs in two distinctive forms: i) calcic augite crystals which are predominantly angular and transparent, are most common above 62 mbsf and ii) sub-calcic pyroxenes (mainly Ca-poor augite, less commonly pigeonite and rare hypersthene) that are translucent-green and often strongly abraded. These pyroxenes characteristically have conspicuous dark-coloured, close-set cleavage planes and exsolution lamellae. The dark coloration of the cleavage planes is due to exsolved opaque oxide, which is sometimes developed so extensively that much of the grain is opaque, making it hard to distinguish unambiguously from some lithic clasts.

Fragments of *volcanic glass* are a major component of samples above 62 mbsf, diminishing markedly below this depth, even though an occasional increase may be observed towards the base of the core at 116.55 mbsf (Smellie, this volume). Volcanic fragments are oxidised tachylite, lava and glass shards; the latter are angular and often strongly vesiculated, essentially unaltered, varying in colour from

Tab. 1 - XRF determinations of major (wt%) and trace elements (ppm) on whole rock samples. Analytical uncertainties is always around 1% for major elements elements but MgO and Na₂O that are determined with a lower accuracy, in the order of 20% and 5% respectively. Analytical precision is estimated to be better than 5% for trace element concentrations greater than 10 ppm. No correction on LOI for iron oxidation or CaCO₃ presence is provided in this data set.

Lithology	Sample	Depth	SiO₂	TiO₂	Al₂O₃	Fe₂O₃tot	MnO	MgO	CaO	Na₂O	K₂O	P₂O₅	LOI	Nb	Zr	Y	Sr	Rb	Ce	Ba	La	Ni	Cr	V	Co	Cu	Zn	Nd	Pb
Sandstone	CRP1- 1	19.26	64.67	1.59	13.54	7.12	0.12	3.72	4.15	2.49	2.23	0.36	3.13	50	308	29	446	74	93	454	45	34	68	129	22	24	81	43	8
Sandstone	CRP1- 2	24.53	70.16	0.76	10.06	4.80	0.09	3.50	4.46	2.42	3.53	0.22	5.84	27	216	18	250	59	56	360	26	32	56	81	15	46	354	24	5
Sandstone	CRP1- 2	26.63	67.46	1.07	11.36	5.53	0.10	3.31	5.05	2.69	3.14	0.28	4.40	36	226	22	412	64	64	386	34	38	77	92	18	17	62	26	7
Sandstone	CRP1- 3	27.51	70.53	0.74	11.05	5.00	0.08	2.95	3.48	2.49	3.31	0.37	4.19	35	232	24	285	76	70	497	32	26	48	77	16	19	61	28	7
Sandstone	CRP1- 3	30.88	70.59	0.82	10.88	4.97	0.08	2.86	3.59	2.51	3.49	0.21	4.40	35	225	22	266	73	72	406	33	25	54	83	16	20	61	26	5
Sandstone	CRP1- 4	33.16	60.02	1.05	10.42	5.33	0.09	3.01	14.69	2.6	2.62	0.17	11.76	35	240	24	833	87	66	419	39	34	74	90	16	31	86	31	11
Diamicton	CRP1- 5	38.26	70.25	0.74	11.67	5.14	0.09	2.70	4.05	2.71	2.46	0.18	3.32	32	261	24	271	75	74	414	34	27	55	100	17	16	64	36	6
Sand	CRP1- 7	43.62	59.00	2.06	12.81	9.09	0.16	3.75	6.37	3.26	3.04	0.46	5.76	64	373	35	481	54	109	418	53	36	85	176	26	20	100	50	3
Sand	CRP1- 7	44.83	62.82	1.67	11.74	8.27	0.14	3.22	5.68	3.06	3.03	0.36	4.61	50	303	29	434	54	90	410	43	31	75	147	24	15	83	41	6
Silty sandstone	CRP1- 8	47.00	58.90	1.89	13.44	9.42	0.17	3.68	5.84	3.44	2.73	0.48	5.25	80	435	40	465	72	134	437	66	26	68	150	24	21	120	60	9
Sandstone	CRP1- 10	54.82	67.76	0.71	12.6	5.37	0.10	3.01	4.35	2.86	2.98	0.25	3.42	32	277	28	280	85	78	447	35	27	56	95	16	18	70	28	10
Sandstone	CRP1- 11	55.85	74.20	0.43	9.96	4.10	0.08	2.59	3.68	2.53	2.32	0.12	2.09	15	202	17	250	63	51	370	25	31	69	81	16	12	45	21	18
Sandstone	CRP1- 12	60.66	74.04	0.66	9.02	4.39	0.09	2.50	4.75	2.30	2.08	0.18	2.96	21	208	18	262	54	55	366	26	40	86	82	16	6	44	21	3
Sandstone	CRP1- 12	60.99	73.22	0.83	9.65	4.33	0.09	2.70	3.92	2.68	2.38	0.20	2.57	25	257	21	281	50	62	339	28	38	102	94	17	6	50	23	2
Sandstone	CRP1- 13	61.88	70.32	1.16	10.05	6.17	0.11	2.81	4.36	2.64	2.10	0.28	3.37	38	319	27	326	54	76	362	41	49	107	116	22	14	67	37	5
Sandstone	CRP1- 13	65.27	75.58	0.37	9.43	3.55	0.07	2.59	3.35	2.50	2.46	0.09	2.92	13	197	16	227	54	37	344	17	33	73	78	14	10	38	18	5
Sandstone	CRP1- 15	72.51	75.45	0.37	9.80	3.30	0.06	2.41	3.26	2.64	2.63	0.09	3.00	13	185	16	234	58	39	355	17	27	67	72	12	10	36	18	3
Fine sand	CRP1- 16	74.40	72.93	0.45	11.15	3.71	0.06	2.33	3.40	2.55	3.29	0.13	3.29	17	182	20	250	73	52	404	21	25	56	71	12	12	46	19	6
Sandstone	CRP1- 17	78.85	69.91	0.44	10.16	6.81	0.12	2.37	5.20	2.57	2.23	0.19	5.72	20	179	22	254	70	52	370	30	25	43	83	16	15	54	23	8
Sandstone	CRP1- 17	79.50	78.74	0.34	8.30	3.09	0.05	1.79	2.50	2.57	2.51	0.11	2.56	13	141	13	213	50	44	275	17	19	38	56	11	5	35	14	3
Black silt	CRP1- 19	85.87	67.75	0.85	11.59	7.66	0.09	2.33	3.97	3.01	2.49	0.24	5.03	36	267	25	326	69	76	415	32	24	43	84	18	14	65	33	8
Sandstone	CRP1- 20	89.14	82.27	0.26	6.81	2.69	0.05	1.82	2.35	2.01	1.68	0.07	1.80	8	124	12	187	42	29	239	15	20	44	59	10	6	28	11	
Sandstone	CRP1- 21	90.72	84.74	0.17	6.15	2.14	0.04	1.47	2.02	1.78	1.44	0.05	1.49	6	87	10	169	40	24	221	11	17	34	45	8	7	24	9	2
Sandstone	CRP1- 21	91.50	81.31	0.31	7.53	2.55	0.05	1.39	2.36	2.27	2.14	0.09	2.67	14	126	13	212	47	31	276	17	14	28	47	8	9	32	17	
Sandstone	CRP1- 23	97.97	65.85	1.00	13.37	6.73	0.11	2.74	3.64	3.30	3.01	0.24	3.43	63	375	39	305	101	121	467	62	20	45	109	16	18	105	54	10
Sandstone	CRP1- 24	102.55	69.69	0.89	11.65	6.09	0.10	2.40	3.28	3.16	2.52	0.21	2.98	55	320	32	303	77	95	407	49	22	47	97	15	13	89	40	5
Sandstone	CRP1- 25	103.10	75.59	0.43	10.14	3.71	0.06	1.97	3.00	2.64	2.34	0.12	1.83	20	168	17	260	64	53	361	25	22	49	67	13	11	42	16	5
Sandstone	CRP1- 26	106.90	71.57	0.57	12.13	4.32	0.07	2.41	3.55	2.78	2.46	0.14	1.99	27	239	24	277	87	64	449	30	24	51	89	15	13	56	27	8
Sandstone	CRP1- 27	109.70	72.58	0.47	11.66	4.14	0.06	2.45	3.52	2.7	2.31	0.11	1.95	17	203	20	272	78	59	428	29	24	55	88	14	12	49	24	7
Sandstone	CRP1- 28	115.20	69.40	0.53	10.34	4.25	0.15	2.29	7.88	2.41	2.28	0.47	5.33	20	226	22	299	74	61	395	30	28	54	88	13	14	46	24	7
Sandstone	CRP1- 29	116.55	78.00	0.26	9.28	2.74	0.06	1.69	2.55	2.54	2.81	0.07	5.25	22	180	16	225	63	44	344	23	18	42	47	9	8	38	18	5
Sandstone	CRP1- 29	117.55	77.16	0.30	9.19	3.07	0.06	2.09	3.21	2.35	2.47	0.09	2.33	10	174	14	237	56	37	360	17	27	55	60	13	10	39	17	2
Diamictite	CRP1- 32	124.83	68.79	0.62	12.66	4.98	0.09	3.06	4.46	2.79	2.40	0.15	2.13	24	233	22	294	86	63	471	31	29	63	99	17	15	58	31	10

brown to pale brown and colourless, However some brown glass is oxidised, largely opaque and transitional to tachylite. Some lava fragments often contain feldspar, pyroxene crystallites or both and generally have a few tiny ovoid vesicles. With the increasing proportion of crystals, vitric clasts grade into intersertal-textured volcanic fragments. A striking feature of glass shards is the limited extent of alteration, smectite products being rare in basic glasses. Brown glass is dominant in most samples, but colourless glass may sometimes become as abundant as the basic varietes (Smellie, this volume). Sandstone lithofacies contain the larger amounts of glassy volcanic fragments, which are rarer among finer sediments (Cape Roberts Science Team, 1998, Tab. 7). The only level in which the distribution of volcanic fragments seems to be related to a syn-eruptive deposit is found at 116.55 mbsf, testified by the occurrence of a tiny, but distinct, layer of peralkaline trachyte pumice.

Minor amounts of green (Mg-hornblende) to brown hornblende (kaersutite), pink titaniferous augite and aegirine are ubiquitous. Sporadic grains of kaersutite, aenigmatite and arfvedsonite are found in samples in which acidic glasses are more abundant, and these are often associated with anorthoclase crystals. Micas (muscovite and biotite) and opaque minerals (Ti-magnetite, ilmenite and sulphides) are not abundant, they represent an almost constant fraction of less than 1% of the grains. Apatite, zircon, pink garnet and monazite are found among accessory grains.

METHODS

Major and trace element concentrations of whole rocks were determined by X-ray fluorescence on powder pellets, using an automated Philips PW 1480 spectrometer with a full matrix correction procedure, using the method of Franzini et al. (1975) and Leoni & Saitta (1976). This method implies the final recalculation to 100% of the analysis. Analytical uncertainties have been evaluated through repeated analyses of internal standards. In this dataset the uncertainty is always around 1% for major elements; the accuracy evaluated through replicated analyses of international standards is better than 3% for major elements except for MgO and Na_2O which are determined with a lower accuracy, of the order of 20% and 5% respectively. Analytical precision is estimated to be better than 5% for trace element concentrations greater than 10 ppm. Although not very accurate for major elements, this method ensures a very good comparison within the dataset, on account of its relatively high precision. Loss on Ignition is determined after ignition at 1 000°C for 1 hour. No correction for iron oxidation or $CaCO_3$ presence was made in this dataset.

Major element mineral chemistry of selected samples was determined at Pisa University using an energy dispersion analyser (EDAX PV 9900) mounted on a Philips XL30 SEM, using the software EDAX DX24 2.11 (1996) that allows microanalytical determinations to be made without external reference standards and ensures faster acquisition of data. This method, however,

recalculates analyses to 100%. Calibration was obtained by using 29 international standards of minerals and glasses, according to the procedure of Leoni et al. (1989). Obtained results show, for major elements, precision and accuracy comparable to those yielded by means of Energy Dispersion Electronic Microprobes. Mean percentile errors, with few exceptions, are between 2% and 4% for absolute concentrations of about 3wt%, and between 0.5% and 2% for absolute concentrations larger than 10wt%. Detection limits range from 0.08 wt% (Fe) to 0.15 wt% (Na). Micro-analyses were performed on polished thin sections splattered with a carbon film 35 nm thick. Instrumental conditions were: acceleration voltage 20Kv, tilt angle 0°, take-off angle 35.16°, counting time 100 s with about 2 700 counts per second, electronic beam diameter 0.2-0.5 µm, window thickness 0.3 µm. Matrix effect correction (ZAF) was obtained using the algorithms of Duncumb & Reed (1968), Philibert (1963) & Reed (1965). To minimise alkali loss, glass grains were analysed with a defocused beam or in "window" mode.

Glasses and minerals were analysed for trace elements at the C.N.R.-CSG laboratory in Pavia (Italy), by laser-ablation microprobe-inductively coupled plasma-mass spectrometry (LAM-ICP-MS) using a UV (266nm) laser probe developed at the Memorial University of Newfoundland, Canada (Jackson et al., 1992) and an "Element (Finnigan MAT) mass spectrometer. Data were reduced using the software "LAMTRACE" by S. Jackson, according to the analytical protocol developed at the Memorial University. Spot diameter varied from 25 µm to 80 µm; the analysed grains were always larger than 200 µm.

GEOCHEMISTRY OF BULK ROCK

A selection of variation diagrams for element abundance is shown in figure 1. Levels down to 62 mbsf exhibit varying and usually higher compatible element contents (Ni, Cr, V, Co). Below this level they decrease sharply then tend to rise regularly to reach values not far from the maximum, close to the bottom of the hole. Minimum values of compatible elements occur at about 90 mbsf (89.14 and 91.5 mbsf) and correspond to finer modes and higher concentrations of SiO_2 as a consequence of the larger amounts of modal quartz (Smellie, this volume). Levels just below (97.97 and 102.5 mbsf) are the most enriched in La, Ce, Rb and Na, and are followed by sandstones showing a regular increase of Ni, Cr, Co and V. The variation diagrams show absolute and relative maxima that strictly correlate with modal variations in the glass and quartz contents. In particular, our absolute maxima of Cr and Ni concentrations occur around 60 mbsf where Smellie (this volume) measured an increase in the glass content and Ehrmann (this volume) found a maximum in smectite abundance in the fine fraction. The absolute maximum of glass and smectite abundance at 43 mbsf (near to the Quaternary-Miocene boundary) coincides with maxima in incompatible elements such as La, Nb, Zr, Ce and Na where also Ti, Co and V also show an absolute maximum. Different concentrations shown by compatible
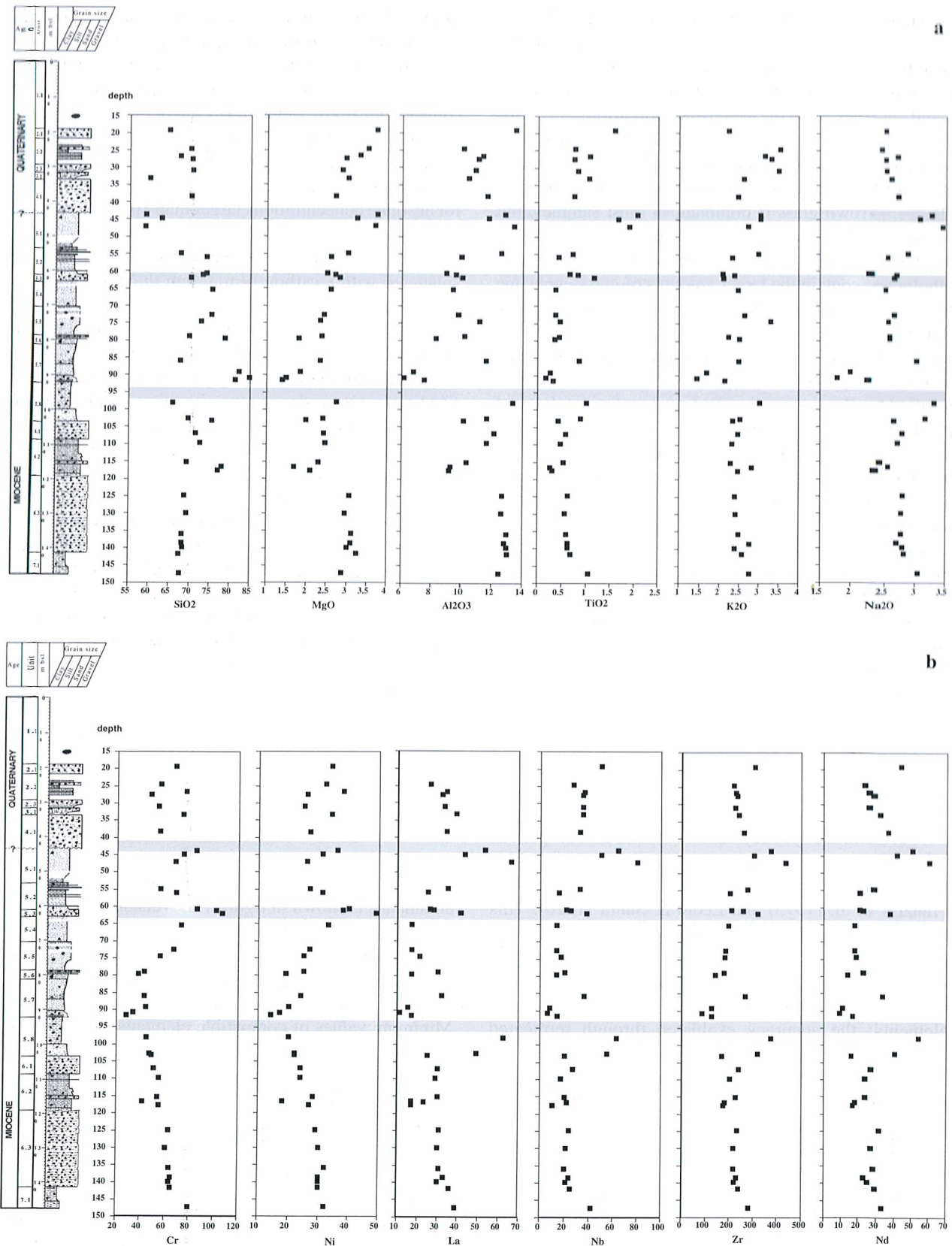
Fig. 1 - a) Variation of major element concentration with depth. Grey bands at 42 and 62 mbsf mark maxima in volcanic glass abundance, that at 95 mbsf correlates with the most fine grained and quartz rich sample with a maximum in rounded/angular ratio of quartz grains. b) Variation of trace element concentration with depth. Grey bands as in figure1a. Note the maximum of Cr content at 62 mbsf and of Nb at 42 mbsf.

and incompatible elements at peaks in modal glass abundance (43.62 and around 60 mbsf; Fig. 1) suggest the occurrence of a larger proportion of evolved volcanic material at 43.62 mbsf; this is supported by modal data

collected from smear slides measured at the drill-site (Cape Roberts Science Team, 1998, Tab. 7).

The third relative maximum in glass content found by Smellie at 116.55 mbsf is not evident in the variation

diagrams (Fig. 1). This is probably due the the dilution effect of quartz which is very abundant at this depth. Samples from 33.6 and 115.2 mbsf show maxima in the CaO content that are due respectively to the occurrence of a carbonate layer and to the presence of sparse carbonate crystals from marbles of metamorphic basement.

Chemical compositions of CRP-1 sandstones have been normalised to the chemistry of possible sources (Ferrar dolerites, Beacon sediments, Granite Harbour Intrusives) in order to find the best possible fitt around the value of unity(Fig. 2). Normalisation data are taken from estimates reported in Roser & Pyne (1989). In spite of the abundance of rounded quartz grains derived from the Beacon Sandstones, the best results are obtained using Granite Harbour Intrusive (GHI) compositions of South Victoria Land(Roser & Pyne, 1989). Normalised patterns are shown in figure 2a where elemental ratios cluster mostly around unity, pointing to a source dominated by Granite Harbour Intrusives, even if Ni, Cr, V, Mg and Nb clearly suggesta provenance from a different source (Fig. 2a).

In figure 2b, the positive covariance of Cr, Ni, Co and V suggests that these elements share the same origin, derived from basaltic glasses or some mafic phase. The same suggestion comes from figure 2c, in which the negative covariance of SiO$_2$ with Cr suggests the presence of a "dilution" trend due to variable amounts of detrital quartz-feldspathic phases, while the most Cr-rich samples around 60 mbsf show the distinct input of a detrital component richer in incompatible elements. On the contrary in figure 2d most Cr-rich sandstones are not the most enriched in Nb, thus excluding the possibility that a Cr-bearing phase may be responsible for a compatible element enrichment, according to the observed Nd distribution coefficients of opaques in alkaline lavas (D'Orazio et al., 1998).

MINERAL CHEMISTRY: MAJOR AND TRACE ELEMENTS

Pyroxenes (Fig. 3) are the most widespread ferro-magnesian minerals. Compositions span from cromian diopside to clino-enstatite; sodic varieties (aegirine-augite) and pigeonite are also common. Enstatites from the Ferrar Group tholeiiitic igneous rocks and augitic clinopyroxenes from the alkalic McMurdo Volcanic Group are the most common pyroxenes (Fig. 3).

Rocks of the Granite Harbour Intrusives may also include pyroxenes, usually as an accessory phase, while amphibole is the commonest mafic mineral in the most widespread granitoids (Armienti et al., 1990a; Allibone, 1993). Augitic pyroxene is more abundant in less evolved gabbros, pyroxenites and their syntectonic metamorphic equivalents (Simpson & Aslund, 1996), and such rocks
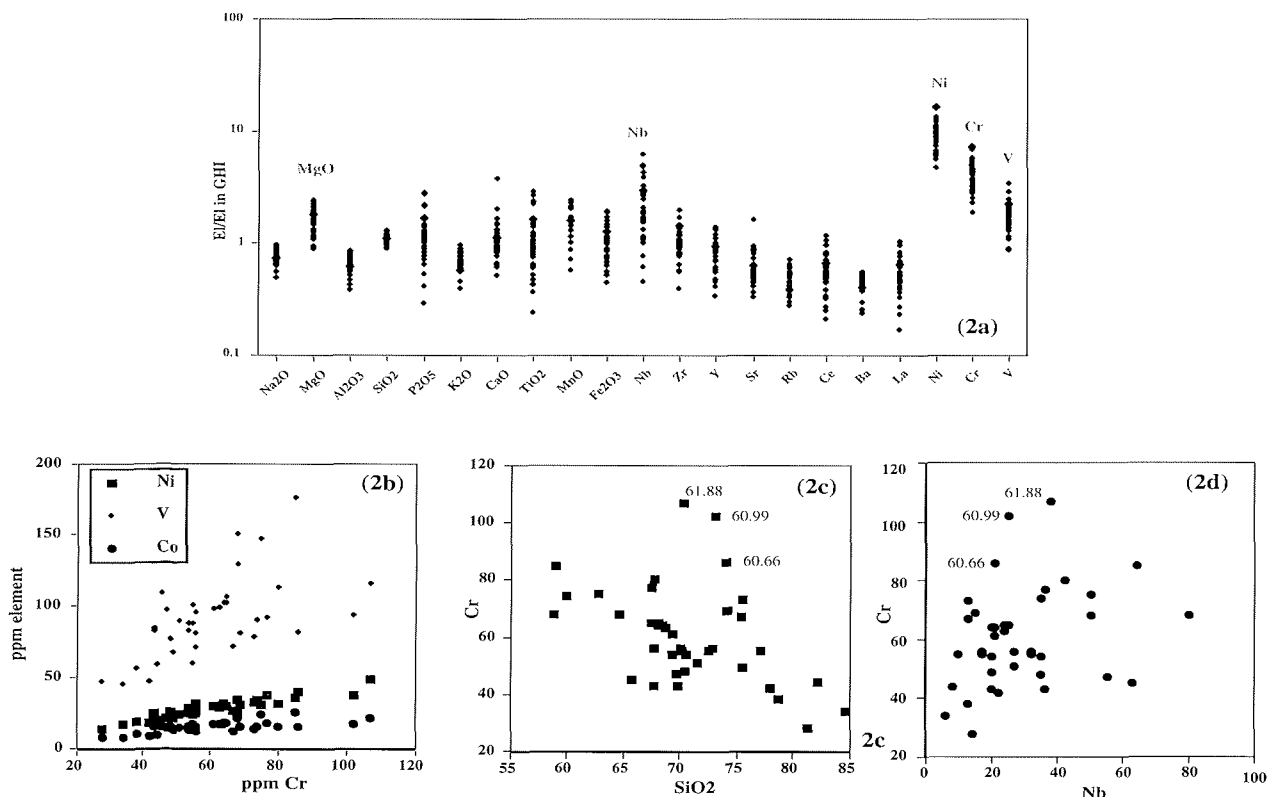

Fig. 2 - a) Ratios between element concentration in CRP-1 sandstones and Granite Harbour Intrusives (see Tab. 1). The grey band marks the unit ratio. Incompatible elements (Ni, Cr, V) and Nb show a distinct source respect to the that prevailing for other elements. *b)* The positive covariance of compatible elements suggests a common source. *c)* Negative covariance of Cr with SiO$_2$ is due to a dilution trend caused by different quartz contents. The highest Cr abundance around 62 mbsf (numbers refer to Tab. 1) correlates with a strong input of Cr bearing phases, mainly the basic glasses, Cr bearing diopside and spinels that are particularly abundant at this depth. *d)* In the Cr *vs* Nb diagram samples richer in Cr are not the richest in Nb. This implies that this latter element is hosted in a distinct phase.
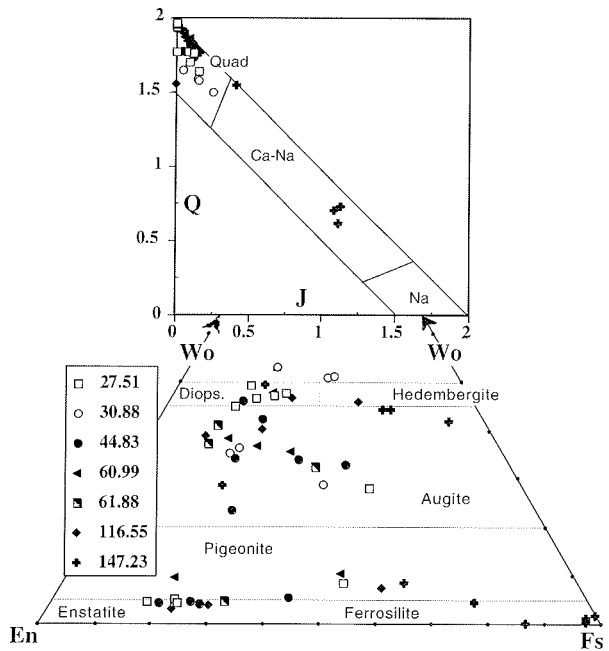
Fig. 3 - Composition of pyroxenes in the Wo-En-Fs triangle. The more iron-rich augitic compositions are typical of evolved pyroxenes of peralkaline lavas. They often exhibit significant amounts of non-quadrilateral components shown in the Q-J inset diagram (Morimoto, 1988).

There is no systematic variation of the proportion of pyroxene with depth; the mineral occurs throughout the core. Table 2 illustrates a selection of minerals that were analysed for major and trace elements by means of SEM based EDS and LAMS. The complete set of major element EDS data is available in the Pangaea Data Base (http//: www.pangaea.de).

Groups of clinopyroxenes from alkaline and peralkaline lavas (Fig. 4) show a humped shape, being enriched in middle rare earth elements (REE), with a marked negative Eu anomaly. Moreover they are distinctly enriched in total REE contents in comparison with pyroxenes from tholeiitic rocks. The latter are clearly depleted in LREE and exhibit a less marked negative Eu anomaly. Among other compatible and incompatible trace elements, the largest variations are observed in Cr content, which is usually higher among augitic pyroxene from the alkaline McMurdo Volcanic Group (Tab. 2). The Nb content of pyroxenes is always less than 5 ppm and therefore they cannot be responsible for the Nb enrichment observed in whole rocks.

Feldspars exhibit a wide variety of compositions from both the high temperature and low temperature series (Fig. 5). They are derived from alkaline rocks of the McMurdo Volcanic Group (An-rich Plagioclase and Anorthoclase-Sanidine) and from the crystalline basement (on the Ab-Or join and Or-poor Albite to Andesine).

Low temperature feldspars are usually found as polycrystalline aggregates with quartz, and are often kaolinitised: they exhibit rounded shapes and exsolution lamellae of Ab. Ca-rich cores of plagioclase varieties of this series are frequently affected by saussuritisation (fine-grained intergrowth of sericite and epidote).

High temperature feldspars are usually less altered than their low temperature counterparts, calcic plagioclase being unaltered, often rich in glass inclusions or partially coated by remnants of basaltic glass. Anorthoclase and sanidine are found as isolated crystals or, more frequently,

could thus represent a possible source of this mineral in the core. However, mineral chemistry data (Armienti, unpubl. data.; Simpson & Aslund, 1996) reveal that in Granite Harbour Intrusives this phase is much poorer in Ti and Al than in both McMurdo and Ferrar volcanics. The Granite Harbour Intrusives can thus be excluded as a significant source of pyroxene in the sandstone of CRP-1. Koettlitz Group metasediments are usually low pressure/high temperature pelitic schists in which pyroxene is absent (Allibone, 1992) and cannot represent a source of pyroxene.
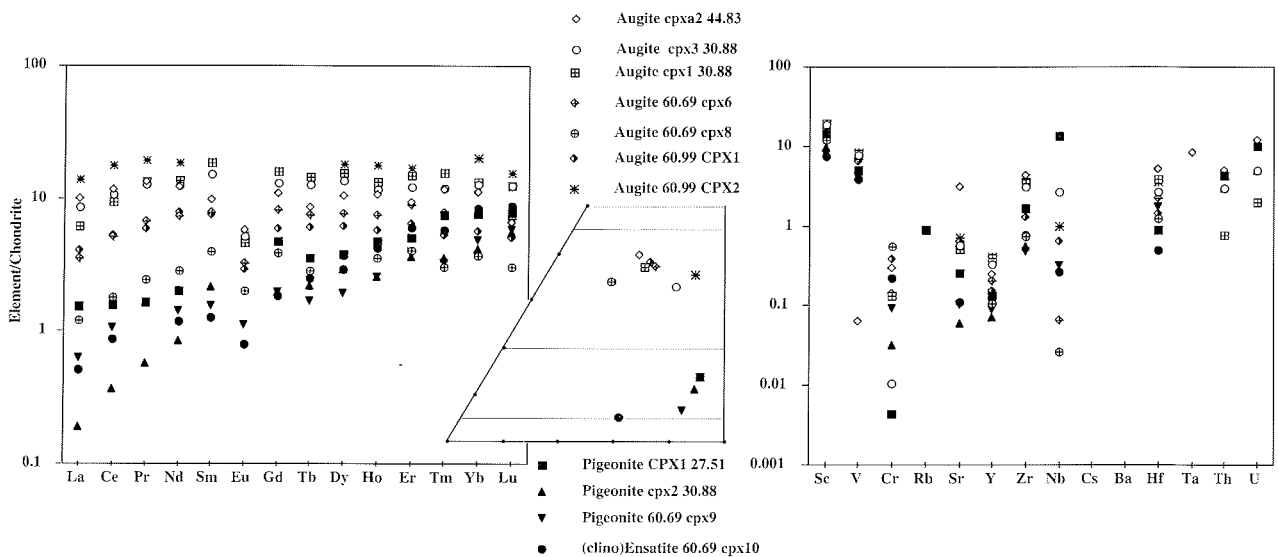

Fig. 4 - Trace element spider diagrams for selected pyroxenes whose major element composition is shown in the inset. Subcalcic pyroxenes are distinctly less enriched in REE ant other incompatible trace elements. Augite is the most Cr-rich variety. Normalisation is respect to chondritic values (Taylor & Gorton, 1977).

Tab. 2 - Pyroxene major (EDS) and trace elements (LAM-ICP-MS). Atomic formula on the basis of 4 cations and 6 oxygens. Classification according to Morimoto (1988).

Depth	27.51	44.83	30.88	30.88	30.88	60.69	60.69	60.69	60.69	60.69	60.99	60.99
Label	cpx 1	cpxa2	cpx3	cpx2	cpx1	cpx5	cpx6	cpx8	cpx9	cpx10	cpx 1	cpx2
SiO_2	49.4	52.6	51.9	51.9	52.3	53.4	52.6	53.1	52.4	54.3	51.8	51.1
TiO_2	0.0	0.4	0.4	0.2	0.5	0.6	0.3	0.3	0.1	0.3	0.4	0.3
Al_2O_3	3.1	1.6	1.8	1.0	1.4	1.6	1.8	1.9	0.9	1.0	2.3	1.7
FeO	23.1	8.8	14.7	23.8	11.6	10.1	10.7	7.4	23.6	17.9	8.6	16.1
MnO	0.7	0.5	0.4	0.6	0.3	0.4	0.4	0.3	0.5	0.3	0.3	0.3
MgO	16.2	16.2	14.7	17.3	15.5	15.9	15.7	19.2	18.8	23.9	16.5	12.9
CaO	6.8	19.6	16.0	5.2	18.2	18.0	18.6	16.9	3.4	2.3	18.8	17.0
Na_2O	0.2	0.3			0.3						0.5	0.3
Cr_2O_3								0.6	0.1		0.5	0.1
V_2O_3												
total	99.5	100.0	100.0	100.0	100.0	100.0	100.0	99.7	99.9	100.0	99.7	99.8
	Pigeonite	Augite	Augite	Pigeonite	Augite	Augite	Augite	Augite	Pigeonite	(clino)Enst.	Augite	Augite
Site T												
Si^{4+}	1.886	1.943	1.956	1.978	1.950	1.985	1.956	1.944	1.987	1.993	1.911	1.944
Al^{3+}	0.114	0.057	0.044	0.022	0.050	0.015	0.044	0.056	0.013	0.007	0.089	0.056
Site M1												
Al^{3+}	0.026	0.014	0.037	0.021	0.009	0.056	0.035	0.025	0.025	0.036	0.012	0.021
Fe^{3+}	0.103	0.041			0.037						0.078	0.038
Ti^{4+}		0.011	0.018	0.012	0.013	0.071	0.001	0.005	0.020		0.011	0.008
Cr^{3+}								0.017	0.003		0.013	0.003
Site M2												
Mg^{2+}	0.051			0.013				0.099	0.095	0.352	0.024	0.000
Fe^{2+}	0.632	0.189	0.340	0.758	0.244	0.270	0.246	0.227	0.748	0.549	0.188	0.274
Mn^{2+}	0.022	0.015	0.014	0.019	0.009	0.012	0.013	0.010	0.017	0.009	0.010	0.010
Ca^{2+}	0.279	0.775	0.646	0.211	0.727	0.718	0.741	0.664	0.140	0.090	0.742	0.693
Na^+	0.015	0.022			0.021						0.036	0.023
Trace elements												
Sc	126	127	161	84	166	130	137	102	69	63	115	159
V	413	537	661	347	677	540	584	423	345	331	552	703
Cr	17	1174	42	127	520		558	2147	364	875	1505	<22
Rb	3											
Sr	3	37	6.7	0.7	6	5.2	6.5	6	1.2	1.3	7.6	8.3
Y	11	21	28	6	34	23	17	8.8	7.5	11	13	35
Zr	9	24	17	3	19		8.9	4.1	2.6	4.3	7	22
Nb	5		1				0.025	0.01	0.12	0.1	0.24	0.37
Cs												
Ba												
Hf	0.16	0.91	0.47		0.68		0.4	0.22	0.31	0.09	0.26	0.65
Ta		0.25										
Th	0.17	0.2	0.12	0.12	0.03							
U	0.1	0.12	0.05	0.05	0.02							
La	0.57	3.71	3.12	0.07	2.27	2.4	1.3	0.44	0.23	0.19	1.5	5.1
Ce	1.51	11.04	10.11	0.35	8.86	10	4.9	1.7	1	0.82	5	17
Pr	0.23	1.87	1.78	0.08	1.84	1.5	0.94	0.34			0.82	2.7
Nd	1.41	8.62	8.86	0.6	9.57	7.9	5.2	2	1	0.83	5.5	13
Sm		2.21	3.43	0.49	4.24	3.3	1.8	0.9	0.35	0.29	1.7	4.3
Eu		0.51	0.46		0.41	0.4	0.29	0.18	0.1	0.071	0.26	0.47
Gd	1.47	3.34	4.05	0.61	4.91	4.2	2.5	1.2	0.61	0.56	1.8	4.9
Tb	0.21	0.51	0.76	0.13	0.87		0.45	0.17	0.1	0.15	0.36	0.84
Dy	1.43	3.92	5.16	1.11	5.8	3.4	2.9	1.4	0.72	1.1	2.3	6.8
Ho	0.42	0.96	1.04	0.23	1.2		0.67	0.32	0.23	0.38	0.51	1.6
Er	1.26	2.3	3	0.91	3.7	2.5	2.2	1	0.99	1.5	1.6	4.2
Tm	0.3	0.46	0.47	0.14	0.62		0.31	0.12	0.13	0.23	0.21	0.63
Yb	1.9	2.79	3.16	1.03	3.29	2.4	1.9	0.93	1.2	2.1	1.4	5
Lu	0.31	0.26	0.5	0.22	0.49		0.28	0.12	0.23	0.35	0.2	0.62

Note: depth refers to the sample, label to the grain analysis.

in fine grained lithic fragments intergrowing with aegirine-augite and minor arfvedsonite.

REE patterns of feldspars are distinctly enriched in LREE with a pronounced positive Eu anomaly. The largest variation in trace element content is exhibited by Ba which varies from a few tens of ppm in plagioclases to 3866 ppm in anorthoclase from highly evolved peralkaline volcanic rocks (Tab. 3).

Glasses. The volcanic glasses and holocrystalline volcanic fragments analysed are derived predominatly from the McMurdo Volcanic Group (Fig. 6). They show the typical bimodal composition of rift-related alkaline volcanism (Daly gap) even though most acidic varieties (peralkaline rhyolite) seem to be lacking in this dataset. There is no depth control on the degree of evolution or alkalinity of glass fragments, and all compositions are represented in every level; the only variability is in the total amount of glass among sand grains. In figure 6 the dashed line separates the field of subalkaline compositions; even though some samples fall in that field, probably

because of alkali loss during analysis or incipient alteration, some of the samples show fresh microcrystalline sub-ophitic intergrowth of pyroxene and feldspar and may be considered as representative of Ferrar Group doleritic rocks. Tholeiitic fragments, however, are scarce and provide a minor contribution to the mode (Smellie, this volume). It is worth noting the occurrence of evolved glasses with $SiO_2 > 57\%$ (Fig. 6), the composition of which is less alkali-rich than the typical values observed in the Erebus Volcanic Province; rather they fall in the field of the intermediate to evolved lavas of northern Victoria Land.

A selection of major and trace elements from glasses is reported in table 4. REE patterns of selected alkaline glass fragments are reported in figure 7 and compared with known basic and evolved rocks from the McMurdo Volcanic Group (Sun & Hanson, 1975; Sun & Hanson, 1976; Kyle, 1990; Armienti et al., 1995). Strongly evolved phonolites from Mt. Erebus are not included in the reference dataset. There is a perfect overlap of composition between the two groups and the glass grains of CRP-1. Even subtle geochemical features of the McMurdo lavas, such as the lack of negative Eu anomalies in intermediate lavas, are reproduced by the sampled population of grains. These Y and major element data allow us to conclude unambiguously that they are derived from the Tertiary volcanic rocks of the Victoria Land area throughout the entire drill-hole.

The Nb content above 190 ppm measured in many intermediate and evolved alkaline glasses allows one to consider them as the main source of this element in the whole rock, in agreement with the maximum Nb content of the samples at 44.83 and 47 mbsf that exhibit the higher
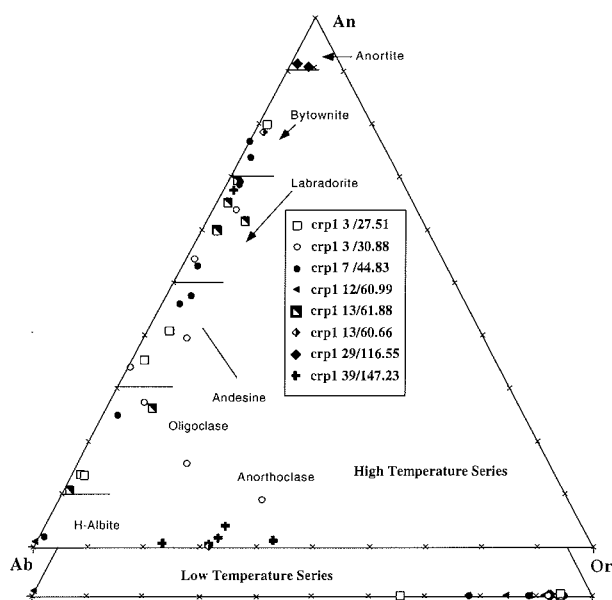
Tab. 3 - Feldspar major (EDS) and trace elements (LAM-ICP-MS).

Depth	27.51	30.88	30.88	30.88	60.66	60.99	60.99
Label	plg c1	1 afsp	9 plg	plg a3	kfsp2	kfsp1	kfsp2
SiO_2	60.67	63.31	51.72	52.06	66.66	64.00	64.50
Al_2O_3	24.78	18.87	29.50	29.78	19.11	19.45	19.28
Fe_2O_3		6.65	2.10		1.35		
MgO					0.26	0.00	
CaO	6.19	1.42	12.51	13.43	0.00		
Na_2O	7.69	4.75	3.51	3.51	7.58	0.67	0.94
K_2O	0.65	4.82	0.66	0.49	5.30	15.88	15.28
Tot.	99.98	99.82	100.00	99.53	100.00	100.00	100.00

Formula recalculated on the basis of 8 oxygens

Si	2.701	2.898	2.370	2.376	2.980	2.957	2.970
Al	1.301	1.019	1.593	1.602	1.007	1.059	1.047
Fe^{3+}	0.000	0.255	0.081	0.000	0.050	0.000	0.000
Mg	0.000	0.000	0.000	0.017	0.000	0.000	0.000
Ca	0.295	0.070	0.614	0.657	0.000	0.000	0.000
Na	0.664	0.422	0.312	0.311	0.657	0.060	0.084
K	0.037	0.281	0.039	0.029	0.302	0.936	0.898
An	29.65	9.00	63.69	65.95	0.00	0.00	0.00
Ab	66.65	54.58	32.29	31.19	68.49	6.03	8.55
Or	3.71	36.43	4.01	2.86	31.51	93.97	91.45
Si+Al+Fe3+	4.002	4.171	4.044	3.979	4.037	4.016	4.016
Na+K+Ca+Mg	0.996	0.773	0.965	1.013	0.959	0.996	0.981

Trace elements

Sc	<5	<5	<9	<11	11		
V	<1	<1	17	9			
Cr	<7	<9	<14	<15			
Rb	154	294	<1.4	8	324	344	366
Sr	574	313	302	309	718	36	97
Y	<0.5	<0.2	<1	1			
Zr	<0.3	0	2	3			
Nb	<0.05	<0.15	<0.2	0			
Cs	13	1.2	<0.7	1.6	5.5	18	11
Ba	185	3866	82	355	2014	453	1003
Hf		0.1	0.09	0.15			
Ta		0.35	<0.17	<0.17			
Pb			2.75		99	159	155
Th	0.03	0.06	0.16	0.12			
U	0.04	0	0	0			
La	49.16	2.37	1.24	5.81	1.7	0.45	
Ce	94.29	1.58	1.97	8.47	2	0.71	
Pr	12.39	0.1	0.23	1	0.18		
Nd	50.22	0.47	0.64	2.35		0.12	
Sm	10.33	<0.12	<0.51	<1			
Eu	3.15	1.47	1.51	2.71	0.69	0.4	0.64
Gd	9.87	<0.32	<0.6	<0.28			
Tb	1.37	<0.03	<0.04	<0.08			
Dy	6.67	0.02	0.06	0.2			
Ho	1.4	<0.02	<0.02	<0.07			
Er	3.65	<0.05	<0.14	<0.2			
Tm	0.47	<0.03	<0.05	<0.5			
Yb	2.87	<0.01	<0.02	<0.05			
Lu	0.38	<0.01	<0.03	<0.35			
				<0.06			

Note: depth refers to the sample, label to the grain analysis; plg-plagioclase, afsp-alkali-feldspar, kfsp-K-feldspar.

□	crp1 3 /27.51
o	crp1 3 /30.88
●	crp1 7 /44.83
◄	crp1 12/60.99
▣	crp1 13/61.88
◈	crp1 13/60.66
◆	crp1 29/116.55
✦	crp1 39/147.23

Fig. 5 - Compositions of low and high temperature feldspar series of CRP-1. Anorthoclase feldspar commonly occur along with aegirine-augite pyroxene, suggesting a common source from peralkaline volcanics of the McMurdo Volcanic Group. More An-rich plagioclase are very fresh and derive from McMurdo Volcanic Group volcanics. Microcline, orthoclase and oligoclase are commonly found in polycrystalline aggregates from the crystalline basement.

content of glass. In fact, even if the Nb content in the kaersutitic amphibole of alkaline lavas reaches a value of 140 ppm (D'Orazio et al., 1998), the total amount of this mineral in the levels most enriched in Nb allows exclusion of a significant role of this mineral in the build up of Nb concentration in whole rocks.

PROVENANCE CONSIDERATIONS AND CONCLUSIONS

The palaeodrainage context of the areas adjacent to the CRP-1 drillsite suggests that Mackay Glacier, Ferrar
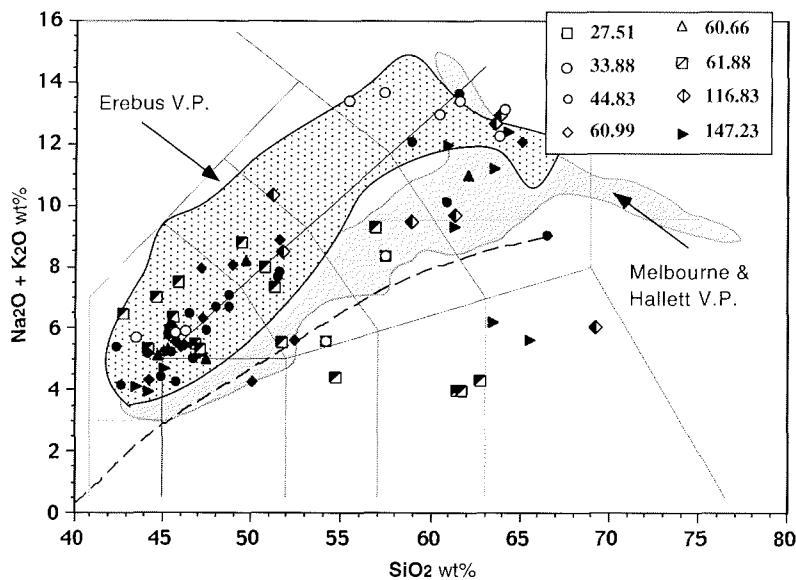
Legend: □ 27.51 △ 60.66 ○ 33.88 ☑ 61.88 ○ 44.83 ◇ 116.83 ◇ 60.99 ▶ 147.23

Erebus V.P.

Melbourne & Hallett V.P.

(y-axis: Na2O + K2O wt%, x-axis: SiO2 wt%)

Fig. 6 - Comparison between the composition of glasses found in CRP-1 sandstones and McMurdo Volcanic Group lavas. The two fields cover the compositions of the Erebus (South Victoria Land) and Melbourne and Hallett Volcanic Provinces. The black dashed curve separates the fields of alkaline and sub-alkaline compositions (Irvine & Baragar, 1971). Compositions falling in the sub-alkaline field are related to tachylitic or polycrystalline aggregates, possibly of Ferrar provenance, even if some alkali loss due to alteration cannot be excluded in a few instances. Source of data: Sun & Hanson (1975), Sun & Hanson (1976), Kyle (1990), Armienti et al. (1990), Armienti & Tripodo (1990), Armienti et al. (1998).

Tab. 4 - Major (EDS) and trace elements (LAM-ICP-MS) of selected glasses.

box	crp1-7	crp1-7	crp1-7	CRP1-13	CRP1-13	CRP1-13	CRP1-13	crp1-29	crp1-29	crp1-29	crp1-29
depth	44.83	44.83	44.83	60.66	60.66	60.99	60.99	116.55	116.55	116.55	116.55
label	gl-a1	gl-a3	gl-4	sc-2	sc-3	gl-1	gl-2	sc-1	pom-1	4	3
SiO_2	46.21	46.91	60.83	47.40	44.69	47.24	51.56	69.23	63.93	61.32	58.95
TiO_2	4.40	4.02	1.79	2.98	4.90	3.29	2.31	0.71	0.66	0.69	0.89
Al_2O_3	15.78	15.52	15.6	16.95	14.95	16.94	17.14	15.44	14.02	17.81	19.27
FeO	12.47	12.73	6.79	9.16	13.07	9.62	10.03	6.83	7.34	8.53	8.82
MnO	0.39		0.25	0.26	0.38	0.36	0.34	0.32	0.00	0.39	0.51
MgO	4.86	4.53	1.29	11.70	10.64	5.22	2.74	0.41	0.19	0.47	0.39
CaO	10.11	11.51	3.08	6.46	5.23	10.32	6.19	0.79	0.75	0.78	1.19
Na_2O	3.51	2.80	5.00	3.46	3.55	4.20	5.61	1.92	7.73	3.79	3.61
K_2O	1.61	1.61	5.13	1.51	1.57	2.08	3.24	4.11	5.20	5.89	5.83
P_2O_5	0.57	0.07			0.97	0.56	0.65				
S								0.07			
Cl	0.05	0.07	0.24	0.11	0.07	0.16	0.18	0.19	0.18	0.33	0.56
Cr_2O_3											

	K-Trachyb.	Alk-bas.	Trachyte	Alk-bas.	Basanite	Tephrite	Phonotephr.	Dacite	Pant. Trac.	Trachyte	Latite
Sc	28	41	38	42	21	32	16	6	4	29	7
V	283	317	346	283	294	252	88	9	4	276	8
Cr	35	98	149	274	33	87	<12	4		10	
Rb	38	27	31	35	26	47	66	112	87	32	120
Sr	840	701	711	664	878	848	681	11	7	854	20
Y	32	39	31	26	29	27	31	63	56	34	75
Zr	323	327	344	201	254	266	397	870	847	225	1029
Nb	76	74	156	59	66	86	117	218	193	61	190
Cs				<2	<2	0.68	0.72	1.5	1	0.6	1.2
Ba	352	384	351	349	529	520	867	25	15	328	147
Hf	7.32	8.1	8.47					19.8	18.5	5.42	22.1
Ta	4.76	4.97	5.32					12.4	11.4	3.64	10.3
Th	5.29	5.53	7.31					16.4	14.8	4.3	15.4
U	1.37	1.83	3.45								
La	52.78	56.71	49.16	40	55	58	79	132.5	120.3	56.2	115
Ce	101.9	115.2	94.29	78	111	107	148	244.2	225.9	108.2	228.8
Pr	12.51	16.17	12.39	9.5	15	13	16	25.13	22.78	14.27	23.37
Nd	53.09	64.48	50.22	41	69	50	59	103	83.02	60.88	78.21
Sm	11.34	14.63	10.33	7.4	14	9.2	10	16.61	15.42	12.25	15.03
Eu	3.09	3.88	3.15	2.5	4.7	2.7	3.5	2.68	2.34	3.64	1.93
Gd	9.06	11.33	9.87	6.4	8.5	6.8	7.7	12.32	10.9	10.33	12.93
Tb	1.24	1.71	1.37	0.96	1.4	0.88	1.1	2.1	1.77	1.23	2.28
Dy	6.67	10.37	6.67	6.3	7.9	5.9	6.2	12.52	10.68	6.68	14.93
Ho	1.18	1.64	1.4	0.97	1.1	1.1	1.3	2.4	1.98	1.23	2.52
Er	3.54	4.94	3.65	3.2	3.4	2.6	3.5	6.46	5.99	3.27	7.84
Tm	0.51	0.56	0.47	0.44	0.32	0.42	0.49	0.92	0.84	0.41	1.1
Yb	3.17	4.95	2.87	2.3	1.6	2.3	3.2	6.05	5.04	2.23	7.81
Lu	0.39	0.53	0.38	0.23	0.26	0.41	0.49	0.83	0.79	0.29	1.07

Note: depth refers to the sample, label to the grain analysis; gl-vesicle free glass, sc-vesiculated basaltic glass, pom-higly vesiculated acidic glass.

Fig. 7 - REE patterns of selected glass grains. Classification is shown in the inset. Patterns perfectly match the known basic and evolved lavas of McMurdo Volcanic Group here represented by the values of rocks from Melbourne, Hallett and Erebus Volcanic Provinces. Some intermediate volcanic compositions lack the negative Eu anomaly like it is commonly observed among McMurdo Volcanics. The strongly fractionated phonolitic rocks from Mt. Erebus are excluded from the dataset due to their characteristic spikes that have not been observed in the analysed glass fragments. Normalisation is respect to chondritic values (Taylor & Gorton, 1977). Source of data: Sun & Hanson (1975), Sun & Hanson (1976), Kyle (1990), Armienti et al. (1990), Armienti & Tripodo (1990), Armienti et al. (1998).
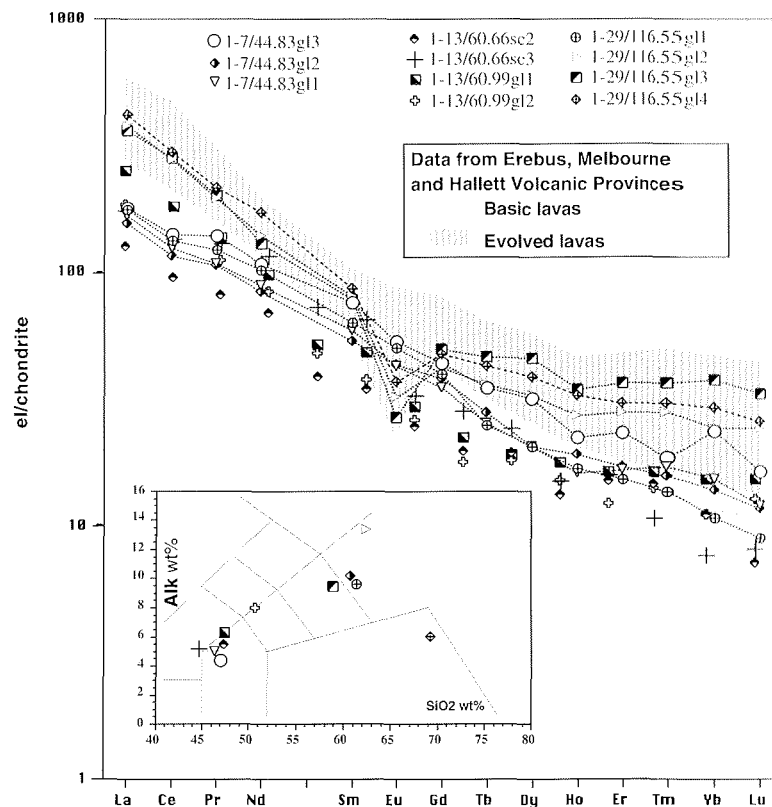
Glacier and other outlet glaciers from the Polar Plateau are the main sources of the sediments. On the basis of geochemical data, it is possible to conclude further that the most abundant detrital grains in CRP-1 sandstones are derived from the Granite Harbour Intrusive units of southern Victoria Land, thus representing the main catchment areas of these glaciers. Petrographic evidence of widespread occurrence of well-rounded quartz and quartz-feldspathic grains also shows that Granite Harbour Intrusives-related grains reached CRP-1 after significant recycling through Palaeozoic sandstones of the Beacon Supergroup. An important contribution to the sandstones of the core is also supplied by a variety of basic to evolved volcanic rocks of the McMurdo Volcanic Group. Input of Ferrar dolerites is revealed by the widespread occurrence of subcalcic pyroxenes which do not obscure the role of McMurdo basic glasses and pyroxenes. The lack of widespred volcanic sequences in the nearby Dry Valleys sector implies that there is significant longshore drift of sediments from the south.

Absolute Ar-Ar dating, together with palaeontological record and magnetostratigraphic data (McIntosh, this volume; Harwood et al., this volume; Roberts et al., this volume) indicates a relation between greater abundance of volcanic glasses and incompatible elements found above 62 mbsf and the widespread alkaline igneous activity in the McMurdo Sound area. In fact, available geochronological data from land areas (Kyle, 1990) date back to 19 Ma a set of subvolcanic units at Mt Morning in southern Victoria Land. However it is clear that a continuous influx of volcanic materials from the McMurdo

Volcanic Group characterises the sedimentation at the drill-site, down to the base ot the hole at 147 mbsl, for which an age from 22 to 24 Ma has been proposed by Harwood et al. (this volume). Even though no volcanic rocks coeval with the base of CRP-1 have been dated in the vicinity of McMurdo Sound, it is still possible to argue that some unknown volcanic centre of this area could have been the source of the observed alkaline volcanics. These materials are usually well preserved, exhibit sharp angular shapes, while their chemistry ensures that in each level they were supplied by a variety of volcanic centres. Moreover, the abundance of vesicles in many glass shards strongly suggests a pyroclastic origin that facilitates wind transportation over large areas of Victoria Land. These considerations indicate that the supply of volcanic particles at CRP-1 is not due to erosion exerted by local glaciers, but mainly to the effects of wind that spreads loose volcanic detritus from exposed areas, over local glaciers or onto marine ice, from where they reached the sedimentation site. The only evidence of tephra linked to an eruption is found at 116.55 mbsf where a thin layer of pumice fragments of identical composition is recorded. In other cases, only a varying extent of areas of exposure of subaerial volcanics, possibly due to periods of more frequent explosive activity, may be inferred from variations in the abundance of volcanic components. The less-pronounced alkali content of some evolved glasses found in the sediments may suggest that some evolved tephra reached the CRP-1 site from North Victoria Land Land, where the onset of Tertiary volcanic activity is documented back to 48 Ma (Tonarini et al., 1997). However, the short time span existing between

the age of the base of CRP-1 and the age of the oldest Tertiary volcanic rocks dated in the McMurdo Sound region does not preclude the possibility that some unknown volcanic centre, less alkaline than those typical of the succeeding period, could have supplied tephra.

ACKNOWLEDGEMENTS

REFERENCES

Allibone H.A., 1992. Low pressure/high temperature metamorphism of Koettlitz Group schists, Taylor Valley and Upperr Ferrar Glacier area, South Victoria Land, Antarctica. *New Zeal. Jour. of Geol. and Geophys.*, 35, 115-127.

Allibone H.A., 1993. Granitoids of the Dry Valleys area, southern Victoria Land, Antarctica: geochemistry and evolution along the early Paleozoic Antarctic Craton margin. *New Zeal. Jour. of Geol. and Geophys.*, 36, 299-316.

Armienti P., Tonarini S., Innocenti F. & Francalanci L., 1995. Cenozoic Magmatism between Priestly and Tucker Glaciers; Northern Victoria Land, Antarctica. VII Int. *Symposium on Antarctic Earth Sciences, Abstract*, 13.

Armienti P., Ghezzo C., Innocenti F., Manetti P., Rocchi S. & Tonarini S., 1990a. Isotope geochemistry and petrology of granitoid suites from the Granite Harbour Intrusives of the Wilson Terrane, North Victoria Land, Antarctica. *European Journal of Mineraolgy*, 2, 103-123.

Armienti P., Civetta L., Innocenti F., Manetti P., Tripodo A., Villari L. & Vita G., 1990b. New petrological and geochemical data on Mt. Melbourne Volcanic Field, Northern Victoria Land, Antarctica. (II Italian Antarctic Expedition). *Mem. Soc. Geol. It.*, 46, 397-424.

Armienti P. & Tripodo A., 1990. Petrography and chemistry of lavas and comagmatic xenoliths of Mt. Rittmann, a volcano discovered during the IV italian expeditin in Northern Victoria Land (Antarctica). *Mem. Soc. Geol. It.*, 46, 427-451.

Armienti P., Francalanci L., Landi P. & Vita G., in press. Age and Geochemistry of volcanic rocks from Daniell Peninsula and Coulman Island, Hallett Volcani Province, Antarctica. In: Thessensshon F. (ed.), *Mariner Volume, Geol Jb.*

Cape Roberts Science Team, 1998. Miocene Strata in CRP-1, Cape Roberts Project, Antarctica. *Terra Antartica*, 5(1), 63-124.

D'Orazio M., Armienti P. & Cerretini S., 1998. Phenocryst/matrix trace-element partition coefficients for hawaiite-trachyte lavas from the Ellittico volcanic sequence (Mt. Etna, Sicily, Italy). *Chemical Geology*, 64.

Duncumb P. & Reed S.J.B., 1968. Quantitative Electron Probe Microanalysis. In: Heinrich K.F.J. (ed.), *NBS Spec Pub.*, 298, 133.

Franzini M., Leoni L. & Saitta M., 1975. Revisione di una metodologia analitica per fluorescenza-X, basata sulla correzione completa degli effetti di matrice. *Rend. Soc. It. Min. Petr.*, 31, 365-378.

Hall B.L., Denton G.H., Lux D.R. & Schlüchter C., 1997. Pliocene Paleonvironment and Antarctic Ice Sheet behavior: evidence from Wright Valley. *Journal of Geology*, 105, 285-294.

Irvine T.N. & Baragar W.R.A., 1971. A guide to the chemical classification of the coommon volcanic rocks. *Canad. J. Earth Sci.*, 8, 523-548.

Jaackson S.E., Longerich H.P., Dunning G.R. & Fryer B.J., 1992. The application of laser-ablation microprobe-inductively coupled plasma-mass spectrometry (LAM-ICP-MS) to in situ trace-element determination in minerlas. *Canadian Mineralogist*, 30, 1049-1064.

Kyle P.R., 1990. McMurdo Volcanic Group, western Ross embayment. In: LeMasurier W.E. & Thomson J.W. (eds.), *Volcanoes of the Antarctic Plate and Southern Oceans*, American Geophysical Union, Antarctic Research Series, 48, 19-25.

Leoni L. & Saitta M., 1976. X-ray fluorescence analyses of 29 trace elements in rock and mineral standard. *Rend. Soc. It. Min. Petr.*, 32, 497-510.

Leoni L., Sbrana A. & Tamponi M., 1989. La microanalisi con il Microscopio Elettronico a Scansione. Il sistema EDAX PV 9900 ed il metodo SUPQ. *Atti Soc. Tosc. Sci. Nat.., Mem. Serie A*, 96, 193-204.

Morimoto N., 1988. Nomenclature of pyroxenes. *Mineralogy and Petrology*, 39, 55-76.

Philibert, 1963. X-Ray and X-Ray Microanalysis. In: Pattee H.H., Cosslett V.E. & Engstrom A. (eds.), *Proc. III Int. Symp.*, Stanford University, Academic New York, 379 p.

Reed, 1965. *Brit. J. Appl. Phys.*, 16, 913 p.

Rose B.P. & Pyne A.R., 1989. Wholerock geochemistry. *DSIR Bulletin*, 245, 175-184.

Simpson G. & Aslund T., 1996. Diorite and gabbro of the Dromedary mafic complex, South Victoria Land, Antarctica. *New Zeal. Jour. of Geol. and Geophys.*, 39, 403-414.

Sun S.S. & Hanson G.N., 1975. Origin of Ross Island basanitoids and limitation upon the etherogeneity of mantle sources for alkali basalts and nephelinites. *Contrib. Mineral. Petrol.*, 52, 77-106.

Sun S.S. & Hanson G.N., 1976. Rare earth evidences of differentiation of McMurdo volcanics, Ross Island, Antarctica. *Contrib. Mineral. Petrol.*, 54, 139-155.

Tonarini S., Rocchi S., Armienti P. & Innocenti F., 1997. Constraints on Timing of Ross Sea Rifting Inferred from Cainozoic Intrusions from Northern Victoria Land, Antarctica. In: Ricci C.A. (ed.), *The Antarctic Region: Geological Evolution and Processes*, Terra Antartica Publication, Siena, 511-521.

Taylor S.R. & Gorton M.P., 1977. Geochemical application of spark source mass spectrography- III. Element sensitivity, precision and accuracy. *Geochimica et Cosmochimica Acta*, 41, 1375-1380.